

25th ABCM International Congress of Mechanical Engineering
October 20-25, 2019, Uberlândia, MG, Brazil

COB-2019-0446

THERMO-HYDRAULIC SENSITIVITY ANALYSIS OF SOLAR AIR HEATER CHANNEL WITH DELTA-WINGLET VORTEX GENERATORS

Daniel Jonas Dezan
André Damiani Rocha
Wallace Gusmão Ferreira

Federal University of ABC – Santo André – SP - Brazil
daniel.dezan@ufabc.edu.br, a.damiani@ufabc.edu.br, wallace.ferreira@ufabc.edu.br

Abstract. *The thermo-hydraulic performance of solar collectors depends on the ability of the working fluid to remove the heat stored on those devices. Basically, the benefits of heat transfer enhancement by using special surface geometries are due to an increase of the convective heat transfer coefficient or/and surface area. The use of modified surfaces reduces the thermal resistance and thus provides an increase of the convective heat transfer coefficient. However, the heat transfer enhancement is always associated with pressure drop increasing. This research deals with the numerical investigation of the thermo-hydraulic performance of flat-plate solar air heaters with delta winglet vortex generators by using Computational Fluid Dynamics. The flow is assumed to be incompressible, turbulent and steady. The $k-\omega$ SST turbulence model is employed to treat the turbulence phenomena. Three rows of delta-winglet pairs are mounted in Common-Flow-Down arrangement in the channel. The Reynolds number, based on hydraulic diameter, is kept constant ($Re_{Dh}=10,000$). It is evident that the amount of the design of experiments to maximize the thermo-hydraulic performance of SAH can be enormous. Thus, it is statistically investigated the effect of the chord, height and angle of attack of three rows of delta-winglet pairs on the averaged Nusselt number and friction factor. For this task, Morris method is used for classifying and ranking the main and interaction effects among the input variables. The Design of Experiments (DoE) was performed by using the Latin Hypercube Sampling algorithm. The results from sensitivity analysis (Morris) indicated that the input parameters affect differently the responses and overall the most important contributors for both heat transfer and pressure drop are c_1 , c_3 , θ_1 , θ_3 . The flow field and heat transfer behavior of the configuration of DWL pairs that produced the best thermo-hydraulic performance are presented and discussed.*

Keywords: *longitudinal vortex generators, delta-winglet vortex generator, solar air heaters, renewable energy, computational fluid dynamics*

1. INTRODUCTION

Over the years, the energy consumption has drastically increased especially due to the world population growth, industrial development and urbanization. Since the continuous use of fossil fuels would eventually lead to the exhaustion, non-conventional energy resources have started playing attention nowadays. In this sense, the plentiful, inexhaustible source and renewable nature of the solar energy becomes it adequate to be used in solar thermal applications.

Solar air heaters (SAHs) are very popular equipment and widely used for applications which require low and moderate temperatures, such as space heating and crop drying. The studies related to thermo-hydraulic performance of those devices has become an interesting area for researches around the world. The great advantages of the solar air heaters, in comparison with solar liquid heaters, are that the SAHs are able to avoid concerns of freezing and, environmental and health hazard risks from the heat transfer fluid (Kabeel et al., 2017). In turn, the most important drawbacks of the SAHs are the low thermal efficiency due to the low convective heat transfer rate between heat transfer fluid and the absorber plate, and high thermal losses to the environment (because of the high temperatures achieved in the absorber plate), (Chamoli et al., 2018), (Sorour and Mottaleb, 1984). Figure 1 illustrates a sketch of the SAH with its main components.

One efficient method to enhance the performance of the SAHs is by increasing the convection heat transfer coefficient between flowing air and absorber plate. The heat transfer enhancement methods applied to SAHs normally include artificial roughness and longitudinal vortex generators (LVGs), and thereby improving the SAHs performance.

It is well known that the use of LVGs is an effective way to improve the heat transfer coefficient in ducts, since the heat transfer enhancement is normally achieved with low pressure penalty. According to Fiebig (1998), the longitudinal vortices are more efficient for heat transfer enhancement than transverse vortices, under the same operating conditions. Another important assessment about LVGs is that the longitudinal vortices enhance heat transfer in steady state flow (Fiebig, 1995).

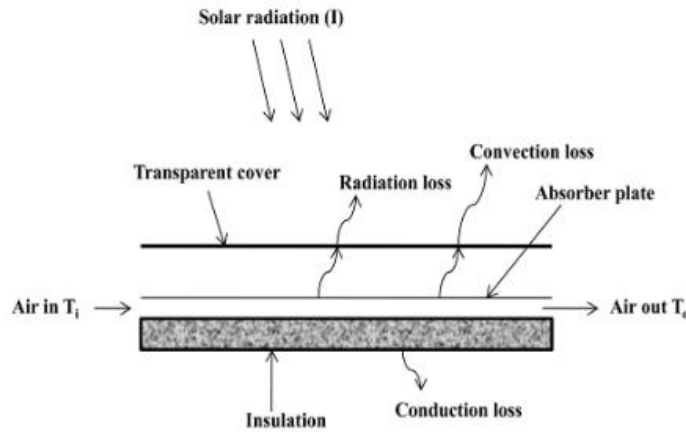


Figure 1. Schematic view of a typical SAH showing the main components. (Rajarajeswari and Sreekumar, 2016)

1.1 Important parameters

The parameters to calculate the heat transfer and pressure drop for a fluid flowing in a channel are dependent of geometrical and flow conditions. The flow can be characterized by Reynolds number and the thermo-hydraulic performance can be predicted by Nusselt number and friction factor. These dimensionless numbers are defined, respectively, as

$$Re_{D_h} = \frac{\rho u_{in} D_h}{\mu} \quad (1)$$

$$Nu = \frac{h D_h}{k} \quad (2)$$

$$f = \frac{2 \Delta P D_h}{\rho u_{in}^2 L} \quad (3)$$

where u_{in} is the mean velocity at the inlet domain, D_h is the hydraulic diameter of the channel, μ is the absolute viscosity of the air, ρ is the density of the air, k is the thermal conductivity, $\Delta P = P_{in} - P_{out}$ is the pressure drop of the channel and L is the length of channel.

1.2 Sensitivity Analysis (SA)

According to Saltelli et al. (2009), Sensitivity Analysis (SA) can be defined as the process to evaluate how uncertainty in the responses of a model can be attributed to different sources of uncertainty in the model variables. In other words, the process can be viewed as a way to understand the influence of each input variable and possible interactions among variables to the output or responses of the model. With that said it is possible reduce (screening) the reasonable number of variables to be controlled or optimized in the process. In the present work it is applied the Morris method (Morris, 1991), based on the Octave implementation adapted from Forrester et al. (2008). With Morris method it is possible to classify the inputs in three groups, i.e.: variables with negligible effects, variables with large linear effects without interactions and inputs having large interaction (or non-linear) effects. Further details and a comprehensive discussion about SA methods can be found in Saltelli et al. (2009) and in the literature review by Borgonovo and Plischke (2016).

2. NUMERICAL METHOD, COMPUTATIONAL DOMAIN AND BOUNDARY CONDITIONS

The equations governing flow were solved using the ANSYS® Fluent 19.1, which is based on finite volume method. The $k-\omega$ SST turbulence model is chosen because of its excellent trade-off between computational costs and accuracy for the purposes of the research.

Figure 2 shows the computational domain and important parameters under investigation. From that, it can be seen that the geometrical parameters are independent from each other. The range of the chord (c), height (h) and angle of attack (θ) of the DWLs are $8 \text{ mm} \leq c \leq 40 \text{ mm}$, $8 \text{ mm} \leq h \leq 21 \text{ mm}$ and $-45^\circ \leq \theta \leq -15^\circ$.

Due to the periodicity in the domain and to save computational time, the periodic boundary condition is applied to the x-y plane, as observed in Figure 3. The bottom wall is assumed to be perfectly insulated (adiabatic wall) and the top

wall (absorber plate) and DWLs are exposed to a uniform heat flux (1000 W/m^2). At inlet and outlet of the numerical domain, constant velocity based on Reynolds number and atmospheric pressure boundary conditions are imposed, respectively. At the solid surfaces (walls and DWLs), the non-slip boundary condition is employed.

The dimensions of the channel are $310\text{mm} \times 120\text{mm} \times 30\text{mm}$ ($L \times W \times H$), $W_c = 30 \text{ mm}$ and the spacing between the half of the DWL chords are $L_a = 30 \text{ mm}$ e $L_b = 75 \text{ mm}$. The length of the entrance and core regions are $L_{\text{entr}} = 60 \text{ mm}$ and $L_{\text{domain}} = 310 \text{ mm}$. The thickness of the DWLs and the Reynolds number are kept constant and equal to 1.20 mm and $10,000$, respectively.

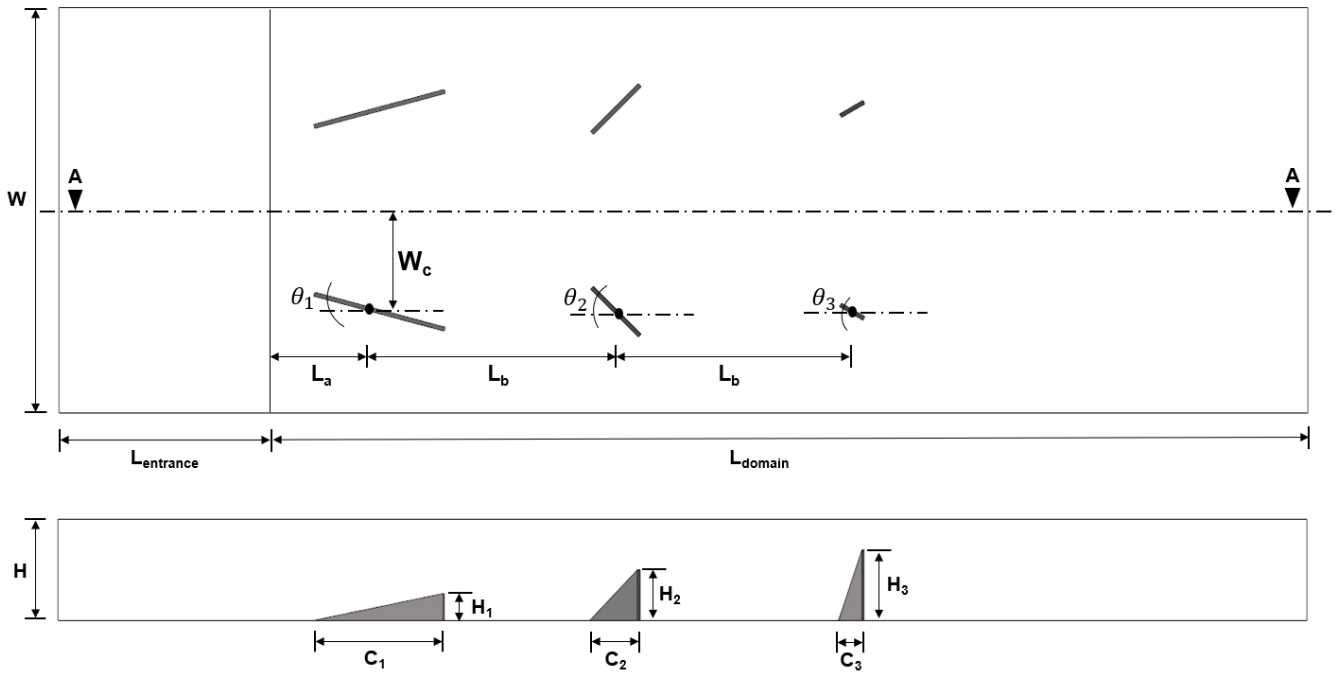


Figure 2: Computational domain and input parameters.

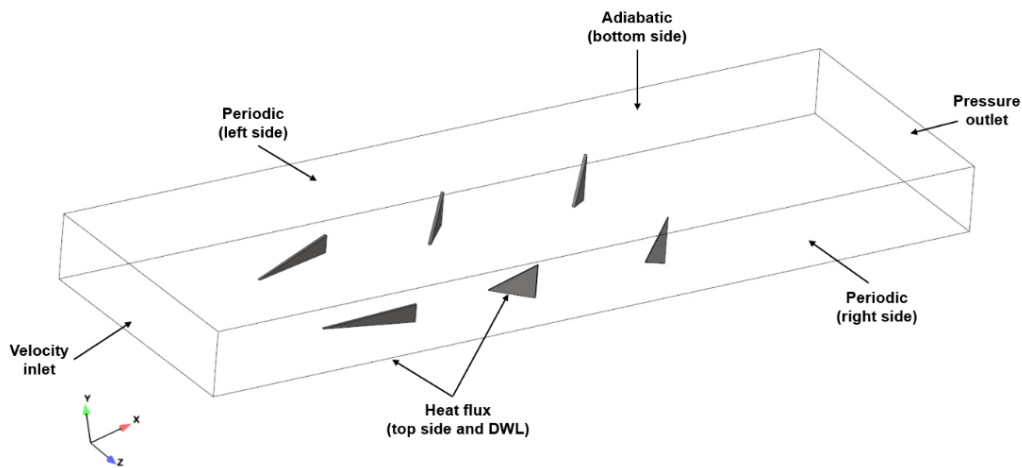


Figure 3: Boundary conditions imposed for the numerical simulations.

Besides that, the turbulence intensity is required at the inlet and outlet domain. In this work, the turbulence intensity is calculated as a function of Reynolds number by using

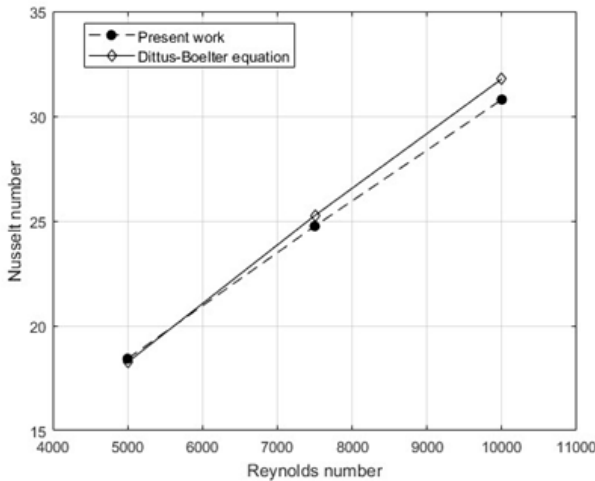
$$I_T = 0.16Re_{Dh}^{-1/8} \quad (4)$$

3. GRID INDEPENDENCY STUDY AND NUMERICAL VALIDATION

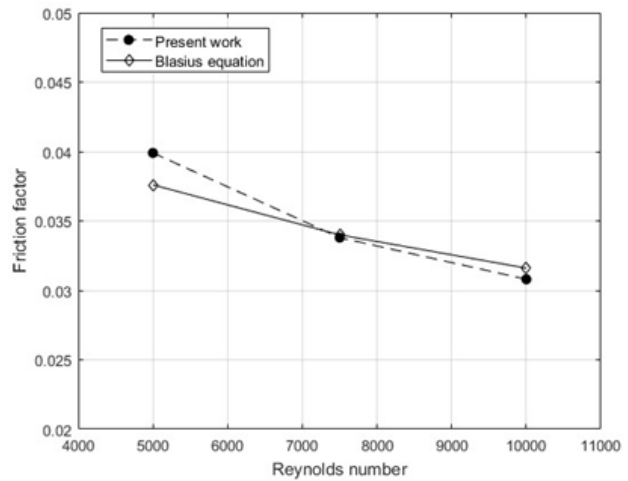
The grid independence test is carried out by using the Grid Convergence Index (GCI) method (Roache, 1994), which is based on generalized Richardson extrapolation. Three mesh sizes are tested to compute the discretization errors. The test is performed for DWL vortex generator with $c_1 = c_2 = c_3 = 40$ mm, $h_1 = h_2 = h_3 = 21$ mm and $\theta_1 = \theta_2 = \theta_3 = -45^\circ$. This case was chosen because it represents a critical flow pattern and thermal characteristics with high swirling flow and heat transfer gradients. The results for friction factor and averaged Nusselt number are depicted in Table 1. In order to validate the numerical procedure, the results for averaged Nusselt number and friction factor by considering a smooth channel were compared to the Dittus-Boelter and Blasius correlations, respectively. As observed in Figure 4, the results from the numerical method are in good agreement with those from the correlations. In general, the numerical results can be considered robust and reliable for the purposes of this research.

Table 1: GCI for the finest mesh in terms of friction factor and averaged Nusselt number.

	Re_{Dh}	Fine Mesh	Intermediate Mesh	Coarse Mesh
Cells number, n		9194467	2940514	1255078
Refinement factor, r		-	1.3278	1.4618
f	5000		0.00174 %	
	7500		0.00184 %	
	10000		0.00256 %	
Nu	5000		0.304 %	
	7500		1.280 %	
	10000		1.630 %	



(a)



(b)

Figure 4. Comparison between CFD predictions and correlations from (a) Dittus-Boelter and (b) Blasius.

4. RESULTS AND DISCUSSION

4.1 Outcomes from Morris method

The SA results based on Morris method are presented in Figures 5 and 6 for both output responses, i.e., averaged Nusselt number and friction factor. Morris plots present the mean value $[\mu]$ and standard deviation $[\sigma]$ of Elementary Effects (EE) for each design variable. Basically $[\mu]$ indicates the main effect (or first order) of each parameter in the model and $[\sigma]$ indicates the higher order effects (nonlinear or interactions). To achieve the reliable statistic results and curve-fitting of the metamodel it was run about 200 numerical simulations. The Design of Experiments (DoE) to run the numerical simulations was performed by using the Latin Hypercube Sampling (Urban and Fricker, 2010; Leary et al., 2003).

As can be observed in Figure 5, the angles of attack and chords of the DWL pairs for the three rows are the main influential variables. In general, the angle of attack and chords of the first row are the most important parameters for heat transfer. By their turns, h_1 , h_2 and h_3 showed low or negligible effects on the response. Those six main variables (c_1 , c_2 , c_3 and θ_1 , θ_2 and θ_3) presented high individual effect (main effect given by the mean, μ) and also large non-linear

interactions among input variables (σ) regarded to heat transfer. On the other hand, in terms of friction factor (Figure 6), the main influential variables are c_1 , c_3 , θ_1 and θ_3 . However, the heights of the first and third row of DWL pairs exerts moderate effect on pressure drop, which is also observed for the parameters c_2 and θ_2 . Thus, in terms of main effects, only the height of the second row of DWL pairs can be neglected for friction factor analysis.

These preliminary sensitivity analysis results indicate that overall the chords and angles of attack of the first and third rows of DWL pairs are the most influential parameters in both responses. The effect of DWL heights showed to be more important to the friction factor as compared to heat transfer. In addition, the height of the second row, h_2 , seems to have negligible effect on both the responses as compared to other design variable effects.

It is worth noting that based on Morris method it is not possible to separate pairwise interactions between two variables but the only that one variable has high or low nonlinear interaction. For example, in case of Figure 5 it is clear that θ_3 has high both main and interaction effects but it is not possible to infer at first glance which variables are interacting with θ_3 . In this sense, Morris method it is useful to provide quick rank input variables, but additional sensitivity and physical investigations must be performed to explain in detail the contribution of each variable in the model responses.

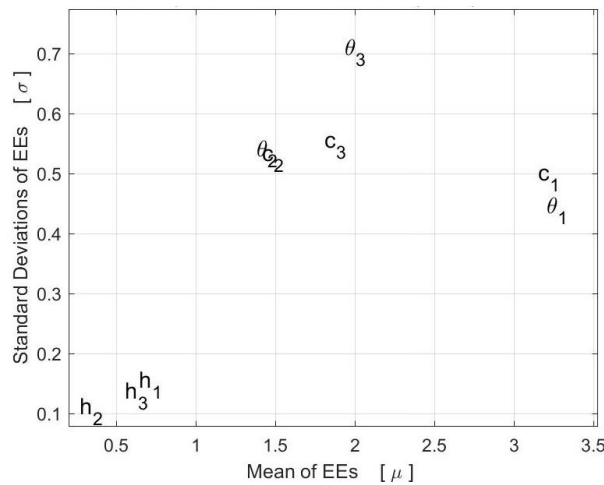


Figure 5. Morris sensitivity plot: main input variables effect, μ versus input variables interaction (nonlinear) effect σ for model responses - averaged Nusselt number.

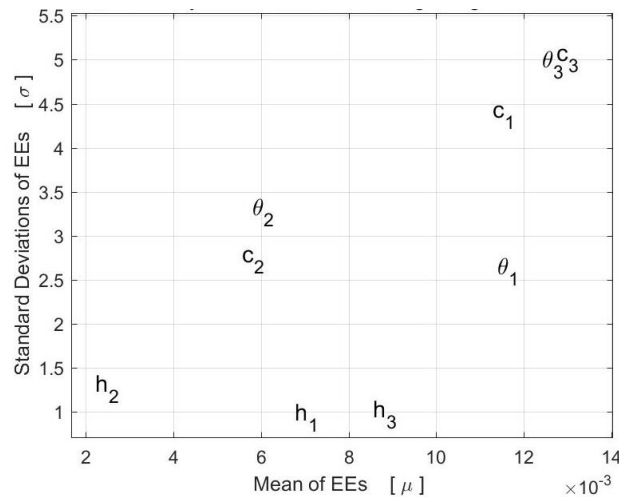


Figure 6. Morris sensitivity plot: main input variables effect, μ versus input variables interaction (nonlinear) effect σ for model responses – friction factor.

4.2 Flow field and heat transfer for Case 1 configuration

The flow field and heat transfer characteristics of Case 1 configuration is investigated in the next paragraphs. The Case 1 is the arrangement that provided the highest thermo-hydraulic performance among all numerical runs. The performance (JF) of the proposed geometry is calculated by comparing the results for the channel with DWLs and without DWLs (smooth channel), according to the equation below

$$JF = \frac{\left(\frac{Nu}{Nu_0}\right)}{\left(\frac{f}{f_0}\right)^{1/3}} \quad (5)$$

where the subscript “0” is referred to the values for smooth channel.

From Table 2, the DWL pairs are not periodically arranged in the domain and the higher values of the geometrical parameters are observed for the second and third rows of DWLs. The heights of the DWLs pairs for the three rows are similar. For this case, the performance of the channel with DWLs is about 13 % higher than that for a smooth channel, which can be considered a substantial enhancement for laminar flows.

Table 2: DWL configuration with the highest thermo-hydraulic performance – Case 1.

	c_1 (mm)	c_2 (mm)	c_3 (mm)	h_1 (mm)	h_2 (mm)	h_3 (mm)	θ_1 (°)	θ_2 (°)	θ_3 (°)	Nu	f	JF
Case 1	8	20	14	8	8	8	-19°	-39°	-44°	39.79	0.0457	1.133

Figure 7 plots the local heat transfer coefficient (h_x) for Case 1 and $Re_{Dh} = 10,000$. It can be seen that values of h_x are higher in the tip of the DWLs and in the regions where the longitudinal vortices are created. Strong longitudinal vortices generated in the second and third rows of DWL pairs and they are very persistent downstream of DWLs. It is important to note that behind the first row of DWLs low heat transfer coefficients are observed, which is not evidenced in the next two rows. This occurs because the incoming flow is accelerated when passes by DWL rows, especially in the hypotenuse of the DWLs. Thus, the incoming flow from the first row of DWLs is again accelerated in the second and third rows, which decreases the recirculation zones right behind the vortex generators, and then increases the local heat transfer coefficient on those regions (see Figure 8). According to Figure 8, the maximum velocity magnitudes increase about 2.5 times higher than the velocity imposed at the inlet of the domain

From Figure 8, it is also observed the main vortices created at the tip of the DWLs due to the pressure difference between front and rear part of the DWLs. Moreover, the longitudinal vortices tend to move away from the absorber plate towards the adiabatic plate as the air flow travels downstream.

The temperature contours at the absorber plate are presented in Figure 9. It was noted only a slight decreasing in the absorber plate temperature in the first row of DWL pairs since weak longitudinal vortices were created in that region. On the other hand, intense vortical structures are generated on second and third rows, which increase the heat transfer rate and decreases the temperature of the plate.

Finally, the results indicated that the use of DWL vortex generators in common-flow-down orientation and not periodically placed in the absorber plate can provide higher thermo-hydraulic performance than the configurations with DWLs periodically arranged in the plate (which is commonly observed in the researches available in the open literature). Furthermore, the current study suggests that an optimization procedure could be used to find optimal geometrical parameters of DWL pairs in order to maximize the performance of a solar air heater channel-type.

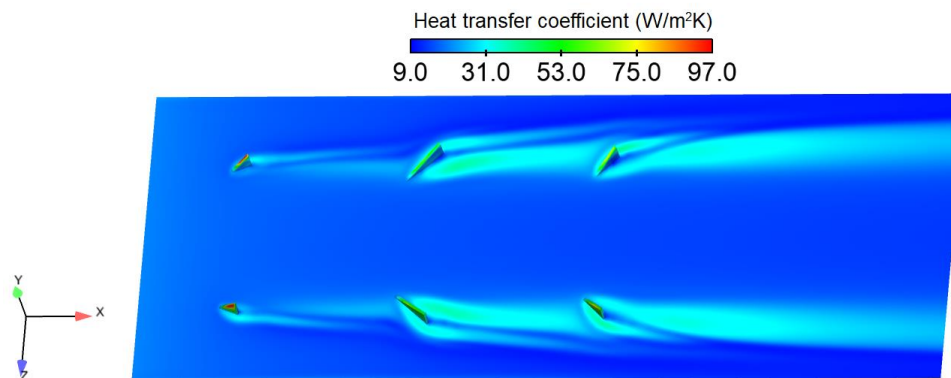


Figure 7. Local heat transfer coefficient at the absorber plate and DWLs – Case 1 configuration.

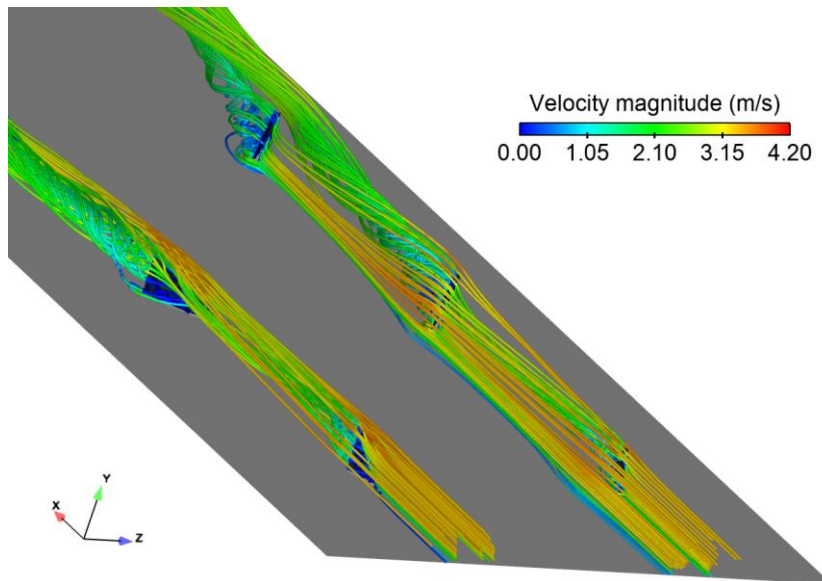


Figure 8. Streamlines along the main flow direction showing the longitudinal vortices generated on each DWL row – Case 1 configuration.

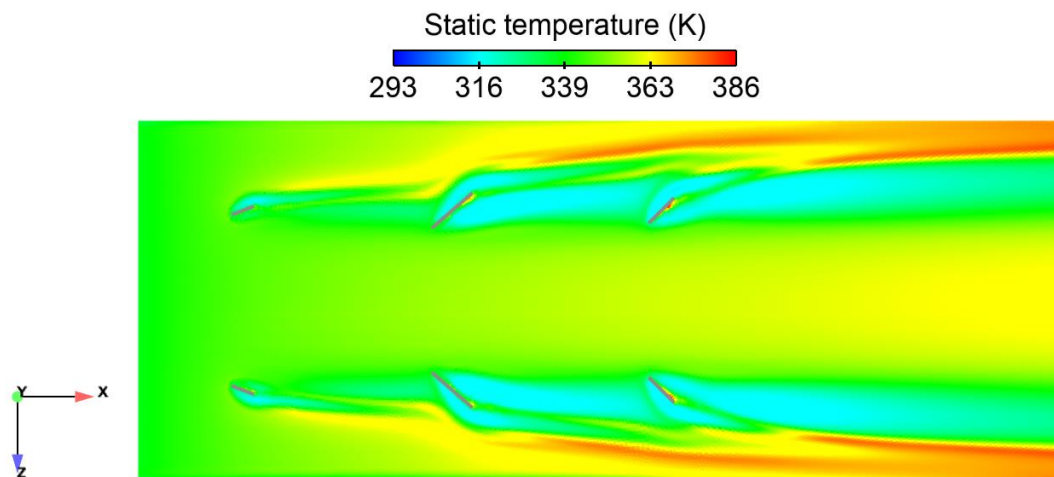


Figure 9. Static temperature in the absorber plate – Case 1 configuration.

5. CONCLUSIONS

The present research numerically investigated the thermo-hydraulic performance of solar air heater channel-type with delta-winglet vortex generators (DWL) by using Computational Fluid Dynamics tool. The effect of nine parameters related to DWLs on thermo-hydraulic performance of the device is also studied for incompressible, turbulent and steady flow. The Reynolds number was kept constant and equal to 10,000. Three rows of DWL pair in common-flow-down arrangement are mounted in the absorber plate and on each row the DWL parameters are varied independently from the other rows, i.e., the arrangement of the DWL pairs are not necessarily periodic in the main flow direction. The Morris method is used for classifying and ranking the main and interaction effects among the input variables for two responses (outputs): averaged Nusselt number and friction factor.

The results from sensitivity analysis (Morris) indicated that the input parameters affect differently the responses and overall the most important contributors for both heat transfer and pressure drop are c_1 , c_3 , θ_1 , θ_3 . With regards to heat enhancement performance, the configuration that presented the highest performance (Case 1) among all numerical simulations was chosen to perform the investigation of the flow patterns and heat transfer characteristics. In the Case 1 configuration the DWL pairs were not periodically mounted in the absorber plate, indicating that an optimization procedure could be used to find other optimal configurations of DWLs, which could not be necessarily mounted in periodic array.

6. ACKNOWLEDGEMENTS

The authors would like to acknowledge Sao Paulo Research Foundation (FAPESP), Grant No. number 2017/06978-3 for the financial and technical support.

7. REFERENCES

- Borgonovo, E. and Plischke, E. 2016. "Sensitivity analysis: A review of recent advances", *European Journal of Operational Research*, Vol. 248, pp. 869-887.
- Chamoli, S., Lu, R., Dexhao, X., Yu, P., 2018. "Thermal performance improvement of a solar air heater fitted with winglet vortex generators", *Solar Energy*, Vol. 159, pp. 966-983.
- Fiebig, M. 1995. "Embedded vortices in internal flow: heat transfer and pressure loss enhancement", *International Journal of Heat and Fluid Flow*, Vol. 16, pp. 376-388.
- Fiebig, M. 1998. "Vortices, generators and heat transfer", *Trans IChemE*, Vol. 76, pp.108-123.
- Forrester, A. I. J., Sobester, A., Keane, A. 2008. *Engineering design via surrogate modeling. A practical guide*, John Willey and Sons.
- Kabeel, A. E., Hamed, M. H., Omara, Z. M., Kandeal, A. W., 2017. "Solar air heaters: Design configurations, improvement methods and applications – A detailed review", *Renewable and Sustainable Energy Reviews*, Vol. 70, pp. 1189-1206.
- Morris, M. D 1991. "Factorial sampling plans for preliminary computational experiments", *Technometrics*, Vol. 33, pp. 161–174.
- Rajarajeswari, K., Sreekumar, A. Matrix solar air heaters – A review, *Renewable and Sustainable Energy Reviews*, Vol. 57, pp. 704-712, 2016.
- Roache, P. J. 1994. Perspective: A method for uniform reporting of grid refinement studies, *Journal of Fluids Engineering*, Vol. 116, pp. 405-413.
- Saltelli, A., Ratto, M., Andres, T., Campolongo, F., Cariboni, J., Gatelli, D., Saisana, M., Tarantola, S. 2009. *Global sensitivity analysis. The primer*, John Willey and Sons.
- Urban, N. M., Fricker, T. E. A comparison of latin hypercube and grid ensemble designs for the multivariate emulation of an earth system model. *Computers & Geosciences*, vol. 36, pp. 746-755, 2010.
- Leary, S., Bashkar, A., Keane, A. Optimal orthogonal array-based latin hypercubes. *Journal of Applied Statistics*, vol. 30, pp. 585-598, 2003.

8. RESPONSIBILITY NOTICE

The authors are the only responsible for the printed material included in this paper.